required and the fact that lateral variations cannot be included in the reflection zone.

4.4 Reflection seismology

4.4.1 The reflection method

Although earthquake seismology and refraction seismology enable scientists to determine gross Earth structures and crustal and upper-mantle structures, reflection seismology is the method used to determine fine details of the shallow structures, usually over small areas. The resolution obtainable with reflection seismology makes it the main method used by oil-exploration companies to map subsurface sedimentary structures. The method has also increasingly been used to obtain new information on the fine structures within the crust and at the crust–mantle boundary.

For land profiles, explosives can be used as a source. Other sources include the *gas exploder*, in which a gas mixture is exploded in a chamber that has a movable bottom plate resting on the ground, and the *vibrator*, in which a steel plate pressed against the ground is vibrated at increasing frequency (in the range 5–60 Hz) for several seconds (up to 30 s for deep crustal reflection profiling). Vibrators require an additional step in the data processing to extract the reflections from the recordings: the cross-correlation of the recordings with the source signal.

Of the many marine sources, the two most frequently used for deep reflection profiling are the *air gun*, in which a bubble of very-high-pressure air is released into the water, and the *explosive cord*. Many air guns are usually used in an array towed behind the shooting ship.

Deconvolution is the process which removes the effects of the source and receiver from the recorded seismograms and allows direct comparison of data recorded with different sources and/or receivers. For the details of the methods of obtaining and correcting seismic-reflection profiles, the reader is again referred to the textbooks on exploration geophysics (e.g., Telford *et al*. 1990; Dobrin and Savit 1988; Yilmaz 2001; Claerbout 1985).

The basic assumption of seismic reflection is that there is a stack of horizontal layers in the crust and mantle, each with a distinct seismic P-wave velocity. Dipping layers, faults and so forth can be included in the method (see Section 4.4.4). P-waves from a surface energy source, which are almost normally incident on the interfaces between these layers, are reflected and can be recorded by *geophones* (vertical-component seismometers) close to the source. Because the rays are close to normal incidence, effectively no S-waves are generated (Fig. 4.39). The P-waves reflected at almost normal incidence are very much smaller in amplitude than the wide-angle reflections near to, and beyond, the critical distance. This fact means that normal-incidence reflections are less easy to recognize than wide-angle reflections and more likely to be obscured by background

noise, and that sophisticated averaging and enhancement techniques must be used to detect reflecting horizons.

4.4.2 A two-layer model

Consider the two-layer model in Fig. 4.34. By application of Pythagoras' theorem, the travel time t for the reflection path SCR is given by Eqs. (4.29) and (4.30) as

$$\begin{aligned} t &= \frac{\mathrm{SC}}{\alpha_1} + \frac{\mathrm{CR}}{\alpha_1} \\ &= \frac{2}{\alpha_1}\sqrt{z_1^2 + \frac{x^2}{4}} \end{aligned}$$

or

$$t^2 = \frac{4z_1^2}{\alpha_1^2} + \frac{x^2}{\alpha_1^2} \tag{4.65}$$

which is the equation of a hyperbola. At normal incidence ($x = 0$), the travel time is $t = t_0$, where

$$t_0 = \frac{2z_1}{\alpha_1} \tag{4.66}$$

This is the two-way normal-incidence time. At large distances ($x \gg z_1$) the travel time (Eq. (4.65)) can be approximated by

$$t \approx \frac{x}{\alpha_1} \tag{4.67}$$

This means that, at large distances, the travel-time curve is asymptotic to the travel time for the direct wave, as illustrated in Fig. 4.32(b). In reflection profiling, since we are dealing with distances much shorter than the critical distance, the travel-time–distance plot is still curved. Notice that, with increasing values of α_1, the hyperbola (Eq. (4.65)) becomes flatter. If travel-time–distance data were obtained from a reflection profile shot over such a model, one way to determine α_1 and z_1 would be to plot not t against x, but t^2 against x^2. Equation (4.65) is then the equation of a straight line with slope $1/\alpha_1^2$ and an intercept on the t^2 axis of $t_0^2 = 4z_1^2/\alpha_1^2$.

The normal-incidence reflection coefficient for P-waves is given by Eq. (4.62). Since normal-incidence reflections have small amplitudes, it is advantageous to average the signals from nearby receivers to enhance the reflections and reduce the background noise. This averaging process is called *stacking*. *Common-depth-point* (CDP) *stacking*, which combines all the recordings of reflections from each subsurface point, is the method usually used. Common-offset stacking, which combines all the recordings with a common offset distance, is less popular. Figure 4.40 shows the layout of shots (or vibrators) and receivers used in CDP reflection profiling. The coverage obtained by any profile is

$$\text{coverage} = \frac{\text{number of receivers}}{\text{twice the shot spacing}} \tag{4.68}$$

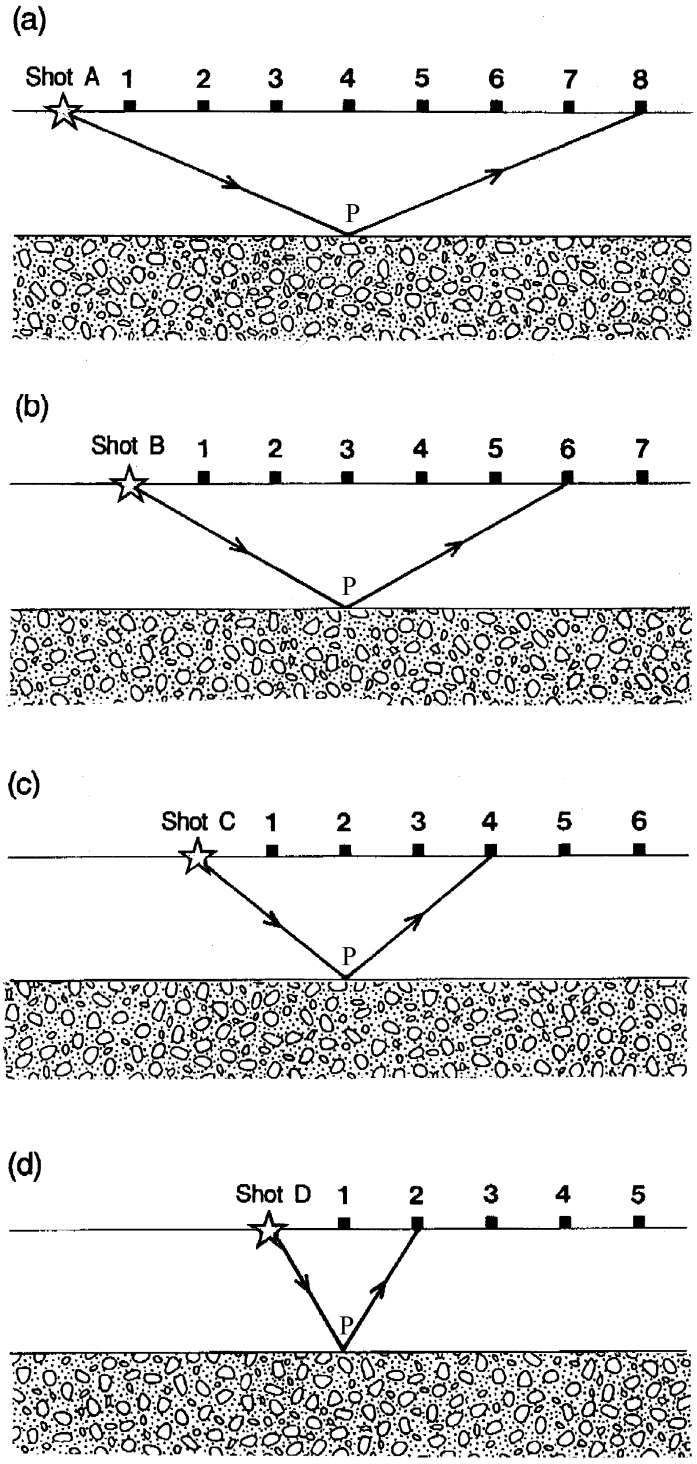

Figure 4.40. Common-depth-point (CDP) reflection profiling. In this example, eight geophones (■) record each shot (★). In (a), shot A is fired and a reflection from a particular point P on the reflector (the interface between the two layers) is recorded by geophone 8. In (b), all the geophones and the shotpoint have been moved one step to the right, and shot B is fired; the reflection from point P is recorded by geophone 6. Similarly, a reflection from P is recorded (c) by geophone 4 when shot C is fired and (d) by geophone 2 when shot D is fired. The four reflections from point P can be stacked (added together after time corrections have been made). In this example, because there are four reflections from each reflecting point on the interface (fewer at the two ends of the profile), there is said to be four-fold coverage. Alternatively, the reflection profile can be described as a four-fold CDP profile.

where the shot spacing is in units of receiver spacing. In the example of Fig. 4.40, the number of receivers is eight and the shot spacing is one. This results in a four-fold coverage. Reflection-profiling systems usually have 48 or 96 recording channels (and hence receivers), which means that 24-, 48-, or 96-fold coverage is possible. The greater the multiplicity of coverage, the better the system is for imaging weak and deep reflectors and the better the final quality of the record section. In practice, receiver spacing of a few tens to hundreds of metres is used, in contrast to the kilometre spacing of refraction surveys.

In order to be able to add all these recordings together to produce a signal reflected from the common depth point, one must first correct them for their different travel times, which are due to their different offset distances. This correction to the travel times is called the *normal-moveout* (NMO) *correction*.

The travel time for the reflected ray in the simple two-layer model of Fig. 4.34 is given by Eq. (4.65). The difference between values of the travel time t at two distances is called the *moveout*, Δt. The moveout can be written

$$\Delta t = \frac{2}{\alpha_1}\sqrt{z_1^2 + \frac{x_\mathrm{a}^2}{4}} - \frac{2}{\alpha_1}\sqrt{z_1^2 + \frac{x_\mathrm{b}^2}{4}} \tag{4.69}$$

where x_a and x_b ($x_\mathrm{a} > x_\mathrm{b}$) are the distances of the two geophones a and b from the shotpoint. The normal moveout Δt_NMO is the moveout for the special case when geophone b is at the shotpoint (i.e., $x_\mathrm{b} = 0$). In this case, and dropping the subscript a, Eq. (4.69) becomes

$$\Delta t_\mathrm{NMO} = \frac{2}{\alpha_1}\sqrt{z_1^2 + \frac{x^2}{4}} - \frac{2z_1}{\alpha_1} \tag{4.70}$$

If we make the assumption that $2z_1 \gg x$, which is generally appropriate for reflection profiling, we can use a binomial expansion for $\sqrt{z_1^2 + x^2/4}$:

$$\begin{aligned}\sqrt{z_1^2 + \frac{x^2}{4}} &= z_1\sqrt{1 + \frac{x^2}{4z_1^2}} \\ &= z_1\left[1 + \left(\frac{x}{2z_1}\right)^2\right]^{1/2} \\ &= z_1\left[1 + \frac{1}{2}\left(\frac{x}{2z_1}\right)^2 - \frac{1}{8}\left(\frac{x}{2z_1}\right)^4 + \frac{1}{16}\left(\frac{x}{2z_1}\right)^6 + \cdots\right]\end{aligned} \tag{4.71}$$

To a first approximation, therefore,

$$\sqrt{z_1^2 + \frac{x^2}{4}} = z_1\left[1 + \frac{1}{2}\left(\frac{x}{2z_1}\right)^2\right] \tag{4.72}$$

Substituting this value into Eq. (4.70) gives a first approximation for the normal moveout Δt_NMO.

$$\begin{aligned}\Delta t_\mathrm{NMO} &= \frac{2z_1}{\alpha_1}\left[1 + \frac{1}{2}\left(\frac{x}{2z_1}\right)^2\right] - \frac{2z_1}{\alpha_1} \\ &= \frac{x^2}{4\alpha_1 z_1}\end{aligned} \tag{4.73}$$

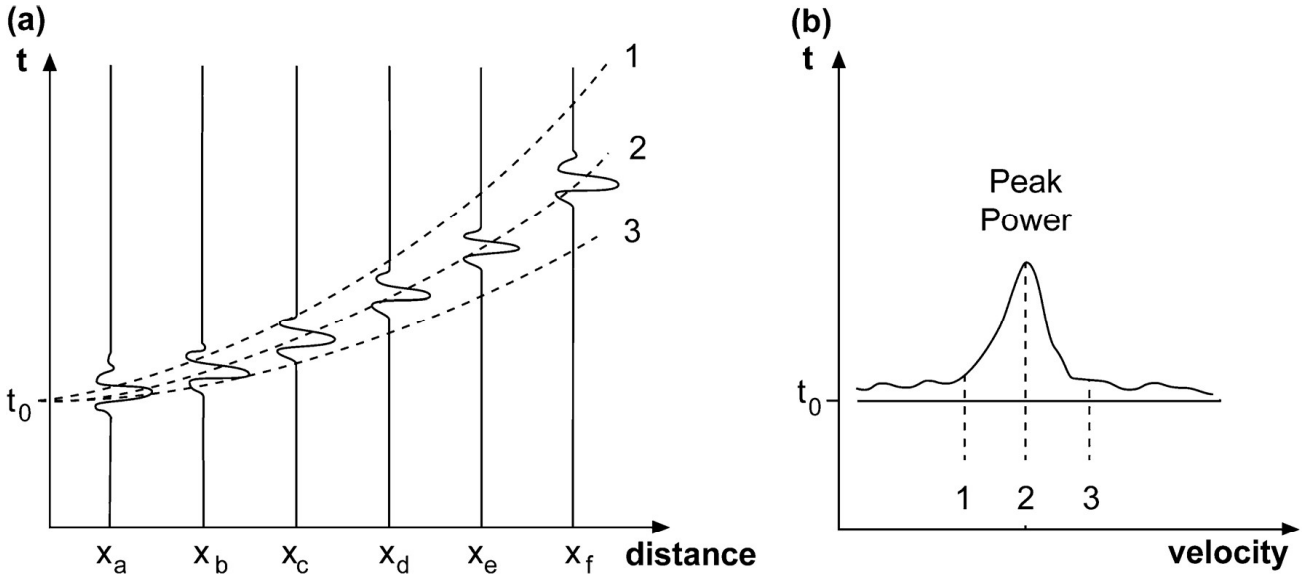

Figure 4.41. (a) Reflections from an interface, recorded at distances x_a, x_b, x_c, x_d, x_e and x_f. Three travel-time curves (1, 2 and 3) are shown for two-way normal-incidence time t_0 and increasing values of velocity. Clearly, curve 2 is the best fit to the reflections. To stack these traces, the NMO correction (Eq. (4.74)) for curve 2 is subtracted from each trace so that the reflections line up with a constant arrival time of t_0. Then the traces can be added to yield a final trace with increased signal-to-noise ratio. (b) The power in the stacked signal is calculated for each value of the stacking velocity and displayed on a time–velocity plot. The velocity which gives the peak value for the power in the stacked signal is then the best stacking velocity for that particular value of t_0. For (a), velocity 2 is best; velocity 1 is too low and velocity 3 too high. (After Taner and Koehler (1969).)

Using Eq. (4.66) for t_0, the two-way normal-incidence time, we obtain an alternative expression for Δt_{NMO}:

$$\Delta t_{\mathrm{NMO}} = \frac{x^2}{2\alpha_1^2 t_0} \tag{4.74}$$

This illustrates again the fact that the reflection time–distance curve is flatter (Δt_{NMO} is smaller) for large velocities and large normal-incidence times. This NMO correction must be subtracted from the travel times for the common-depth-point recordings. The effect of this correction is to line up all the reflections from each point P with the same arrival time t_0 so that they can be stacked (added together) to produce one trace. This procedure works well when we are using a model for which α_1 and z_1 are known, but in practice we do not know them: they are precisely the unknowns which we would like to determine from the reflections! This difficulty is overcome by the bootstrap technique illustrated in Fig. 4.41. A set of arrivals is identified as reflections from point P if their travel times fall on a hyperbola. Successive values of α_1 and t_0 are tried until a combination defining a hyperbola that gives a good fit to the travel times is found. These values α_1 and